

● *Original Contribution*

## THE USE OF THE WAVELET TRANSFORM TO DESCRIBE EMBOLIC SIGNALS

NIZAMETTIN AYDIN,\* SOUNDRIE PADAYACHEE<sup>†</sup> and HUGH S. MARKUS\*

\*Department of Clinical Neurosciences, Guy's King's and St. Thomas' School of Medicine and Institute of Psychiatry, London, UK; and <sup>†</sup>Ultrasonic Angiology Lab, Guy's Hospital, London, UK

**Abstract**—A number of methods to detect cerebral emboli and differentiate them from artefacts using Doppler ultrasound have been described in the literature. In most, Fourier transform-based (FT) spectral analysis has been used. The FT is not ideally suited to analysis of short-duration embolic signals due to an inherent trade-off between temporal and frequency resolution. An alternative approach that might be expected to describe embolic signals well is the wavelet transform. Wavelets are ideally suited for the analysis of sudden short-duration signal changes. Therefore, we have implemented a wavelet-based analysis and compared the results of this with a conventional FFT-based analysis. The temporal resolution, as measured by the half-width maximum, was significantly better for the continuous wavelet transform (CWT), mean (SD) 8.40 (8.82) ms, compared with the 128-point FFT, 12.92 (9.70) ms, and 64-point FFT, 10.80 (5.69) ms. Time localization of the CWT for the embolic signal was also significantly better than the FFT. The wavelet transform appears well suited to the analysis of embolic signals offering superior time resolution and time localization to the FFT. © 1999 World Federation for Ultrasound in Medicine & Biology.

**Key Words:** Fast Fourier transform, Wavelet transform, Cerebral embolism, Ultrasonics, Time localization.

### INTRODUCTION

Asymptomatic circulating cerebral emboli can be detected by transcranial Doppler ultrasound (Spencer et al. 1990). Emboli passing through the sample volume result in a short-duration transient increase in intensity that is maximum across a narrow frequency range (Markus and Tegeler 1995). In certain conditions, such as carotid artery stenosis, asymptomatic embolic signals appear to be markers of increased stroke risk and may be useful in patient management (Markus and Harrison 1995). A major problem with clinical implementation of the technique is the lack of a reliable automated system of embolic signal detection. Recordings in patients may need to take one hour or more in duration, and analyzing the spectra visually is time-consuming and subject to observer fatigue and error. Any processing method that improves the embolic signal-to-background blood signal ratio (EBR), and, therefore, the conspicuity of the embolic signal, will improve the performance of an automated system. Although interobserver reproducibility

studies have demonstrated that there is an overall high level of agreement in identifying embolic signals, this is poorest for embolic signals of low relative intensity (Markus et al. 1997). Agreement would be improved by any method of signal analysis that improves the embolic signal-to-noise ratio.

An ideal signal processing approach for embolic signal detection will have both high temporal resolution and maximize the EBR. In almost all studies of embolic signal detection to date, Fourier transform (FT)-based spectral analysis has been used. In some respects, the FT is not ideally suited to analysis of short-duration embolic signals due to an inherent trade-off between temporal and frequency resolution. These difficulties have led to an attempt to improve temporal resolution using an alternative analysis tool, the Wigner distribution, which has higher time-frequency resolution (Smith et al. 1994). An alternative approach is the wavelet transform, which would be expected to provide a high temporal resolution, being ideally suited for the analysis of sudden short-duration signal changes (Rioul and Vetterli 1991). We, therefore, implemented a wavelet-based analysis for analyzing embolic signals and have compared the results of this with a conventional FFT-based analysis. We examined their relative performance in the analysis of embolic signals from patients with carotid stenosis. The signals in such patients, which are believed to

(Received 8 January 1998; in final form 29 March 1999)

Address for correspondence: Dr. Nizamettin Aydin, Department of Clinical Neurosciences, Institute of Psychiatry, De Crespigny Park, Denmark Hill, London SE5 8AF UK. E-mail: nizamettin.aydin@kcl.ac.uk

result from solid emboli, are of lower intensity than those found in patients with prosthetic heart valves and during cardiopulmonary bypass when the majority are thought to result from gaseous emboli (Grosset et al. 1993). They are, therefore, more difficult to detect and differentiate from artefacts and background Doppler speckle, and this represents a situation where an improved signal-processing approach might have particular benefit.

#### Wavelet transform and time-scale analysis

The wavelet transform (WT) is being increasingly applied, in fields ranging from communications to medicine (Rioul and Vetterli 1991; Akay 1995; Chan et al. 1997), to analyze signals with transient or nonstationary components. Nonstationary means that the frequency content of the signal may change over time and the onset of changes in the signal cannot be predicted in advance. Embolic signals, which are transient-like and of very short duration, fit the definition of nonstationary signals. Like the fast Fourier transform (FFT)-based time-frequency representation, a complete WT process creates a 2 (or 3)-dimensional representation with description of time, wavelet scale (1/frequency), and amplitude of the WT coefficients. The WT decomposes a time series into time-scale space and enables one to determine both dominant modes of variability and how those modes vary in time. The continuous wavelet transform (CWT) is performed by projecting a signal  $s(t)$  onto a family of zero-mean functions (the wavelets) deduced from an elementary function  $\Psi(t)$  (the mother wavelet) by translations and dilations. It is given by:

$$W(a, b) = \frac{1}{\sqrt{|a|}} \int_{-\infty}^{+\infty} s(t) \psi^* \left( \frac{t-b}{a} \right) dt$$

$$a \in \mathbb{R}^+ - \{0\}, b \in \mathbb{R}, \quad (1)$$

where  $*$  denotes the complex conjugate,  $\Psi^*(t)$  is the analyzing wavelet. The variable  $a$  ( $> 0$ ) is the scale factor and controls the scale of the wavelet, so that taking  $|a| > 1$  dilates the wavelet  $\Psi$  and taking  $|a| < 1$  compresses  $\Psi$ . The variable  $b$  is the time translation factor and controls the position of the wavelet. The wavelet transform is characterized by the following properties:

1. It is a linear transformation,
2. it is covariant under translations:

$$s(t) \rightarrow s(t-u) \quad W(a, b) \rightarrow W(a, b-u), \quad (2)$$

and

3. it is covariant under dilations:

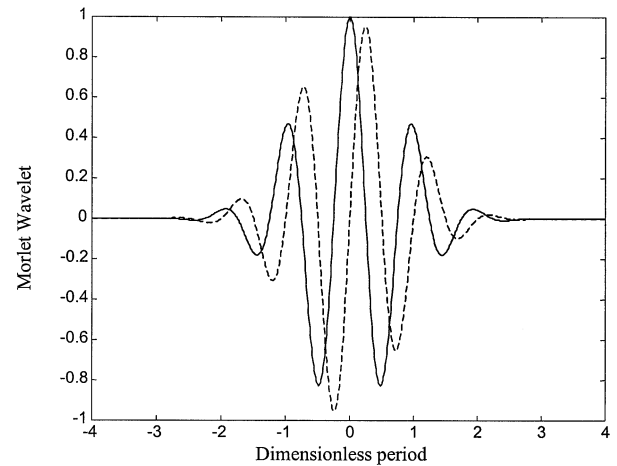


Fig. 1. Real (solid) and imaginary (dashed) parts of the Morlet wavelet.

$$s(t) \rightarrow s(kt) \quad W(a, b) \rightarrow \frac{1}{\sqrt{k}} W(ka, kb). \quad (3)$$

The basic difference between the WT and the FFT is that when the scale factor  $a$  is changed, the duration and the bandwidth of the wavelet are both changed, but its shape remains the same. The CWT uses short windows at high frequencies and long windows at low frequencies, in contrast to the FFT, which uses a single analysis window. This partially overcomes the time-resolution limitation of the FFT. The bandwidth  $B$  is proportional to the frequency  $\nu$ . The CWT can also be assumed as a filter bank analysis composed of band-pass filters with constant relative bandwidth.

If  $W(a, b)$  is the WT of a signal  $s(t)$ , then  $s(t)$  can be restored using the formula:

$$s(t) = \frac{1}{C_\psi} \int_{-\infty}^{+\infty} \int_{-\infty}^{+\infty} W(a, b) \psi \left( \frac{t-b}{a} \right) \frac{da db}{a^2}, \quad (4)$$

providing that the Fourier transform of wavelet  $\psi(t)$ , denoted  $\Psi(\nu)$  satisfies the following admissibility condition:

$$C_\psi = \int_{-\infty}^{+\infty} \frac{|\Psi(\nu)|^2}{\nu} d\nu < \infty, \quad (5)$$

which shows that  $\Psi(t)$ , has to oscillate and decay. One of the original wavelet functions is the Morlet wavelet (Martinet et al. 1986), which is a locally periodic wavetrain. It is obtained by taking a complex sine wave,

and localizing it with a Gaussian envelope (Fig. 1). Analytically, a nonoscillatory function must be subtracted so that the admissibility condition is satisfied. For a sine wave of unit frequency inside an envelope of width  $z_0/\pi$ , it is defined as:

$$\psi(t) = (\cos 2\pi t + i \sin 2\pi t)e^{-2t^2\pi^2/z_0^2} - e^{-z_0^2/2-2t^2\pi^2/z_0^2}. \quad (6)$$

The selection of  $z_0$  reflects a compromise between localization in time and in frequency. A  $z_0$  value of 5 to 6 is recommended in practice (Farge 1992).

## METHOD

A total of 50 consecutive embolic signals from 5 patients with symptomatic carotid stenosis were used for analysis. For inclusion, 2 experienced observers had to agree that the signal was an embolic signal using standard criteria (Ringlestein *et al.* 1998). In addition, a second group of 10 embolic signals of particularly low intensity were evaluated. All had been recorded using a commercially available transcranial Doppler system (EME Pioneer TC4040) with a 2MHz transducer. Recordings were made from the ipsilateral middle cerebral artery using an axial sample volume of 5 mm. Using proprietary SoundTrak<sup>®</sup> software, the FFT spectra containing the embolic signal and the accompanying time-domain audio data were saved to disk. Inside the record, the data are stored as a sequence of sample pairs. Each sample pair at sample time  $n$  consists of an in-phase and quadrature component  $s_i[n]$  and  $s_q[n]$ , sampled once each pulse-repetition frequency (7150 Hz) period. The quadrature data are sampled 90° after the in-phase data. The quadrature sound track data were then exported to a PC for signal analysis using a Matlab program. The sampling frequency of these signals was 7150 Hz and the data length was 2048 point (286 ms). The data were prepared to include embolic signals at the first 143 ms part of the total recordings. The second 143 ms of the data were used to calculate average background Doppler ultrasound power.

The data were analyzed using both the FFT and the CWT. The recorded quadrature signals were converted into directional format by applying the Hilbert transform process (Aydin *et al.* 1994). After obtaining directional Doppler signals, successive groups of 128 and 64 sample points (17.9 ms and 8.95 ms, respectively) with a 99% overlap ratio (127 and 63 points) were taken and data matrices having  $128 \times 2048$  and  $64 \times 2048$  samples, respectively, were created for subsequent 128- and 64-point FFT analysis. To include the last 127 and 63 sample points for FFT analysis, 127 and 63 zeros were added as necessary samples. Both 128- and 64-point

FFTs preceded by 128- and 64-point Hanning windows, respectively, were applied. These processes produce  $128 \times 2048$  and  $64 \times 2048$  point data matrices, respectively, representing time-frequency distribution of a directional Doppler signal.

For CWT analysis, a 64-scale WT using Morlet wavelet was applied to both forward and reverse signals, producing a total of  $128 \times 2048$  data array, representing the time-scale distribution of the signals.

The time-frequency representation of embolic signals using FFT and CWT was compared by calculating EBR, half width maximum (HWM), and embolic signal onset (ESO). For each signal analysis method, the HWM of the time-intensity curve for the embolic signal was measured as an estimate of the temporal resolution of the methods. For time resolution, the time-frequency/scale distribution was integrated over all frequencies/scales. This process should, ideally, result in the instantaneous power of the signal (Williams *et al.* 1997). Then, the HWM for the time resolution was defined as the temporal distance between the point at which power reached half maximum and the point at which it fell to half maximum. This is an indication of the variability of temporal resolution as a function of a certain FFT/CWT parameter considered. The accuracy with which each method described the position of the embolic signal in time was estimated by measurement of the ESO, which was measured at 1 tenth of the maximum instantaneous power. The ESO indicates how the time localization properties of the transforms are influenced by the transform parameters considered. These were compared with the ESO values estimated from the directional time-domain signal. This was taken as reference and the ESO values for the FFT and CWT were found. The EBR was defined as:

$$EBR = 10 \log \frac{A_{\text{peak}}}{B_{\text{avg}}}, \quad (7)$$

where  $A_{\text{peak}}$  is the power at frequency (scale for the WT) with maximum intensity (1 for the normalized data) during the first half of the data record, and  $B_{\text{avg}}$  is the average power of the background intensity. The latter was calculated by time and frequency/scale averaging of the time-frequency/scale analysis results (Torrence and Compo 1998), using the second half of the total data:

$$B_{\text{avg}} = \frac{1}{t_2 - t_1} \sum_{t=t_1}^{t_2} \frac{1}{N} \sum_{\nu=1}^N S(t, \nu), \quad (8)$$

where  $S(t, \nu)$  is the 2-D time-frequency/scale distribution of the Doppler signal and  $N$  is the number of frequency/

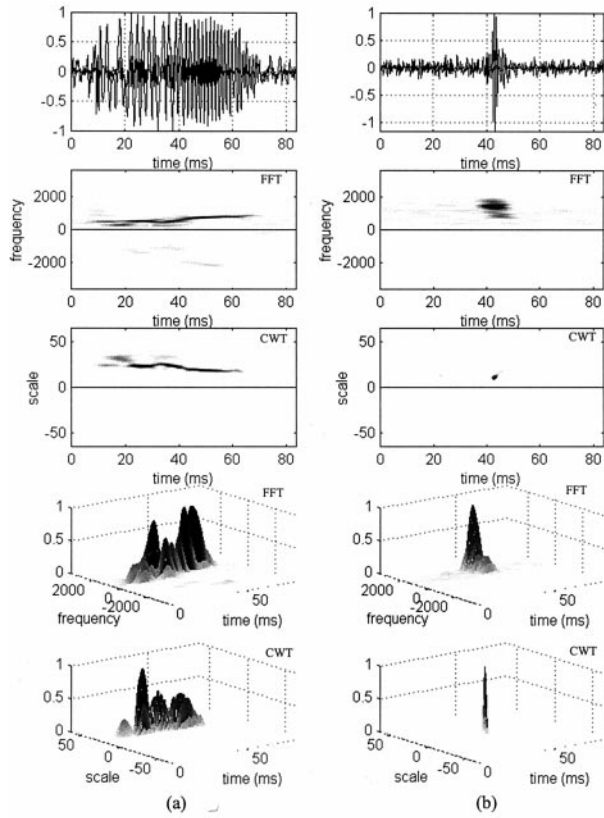


Fig. 2. (a) Long- and (b) short-duration embolic signals and corresponding 2-D and 3-D intensity plots of the FFT and the CWT results (– indicates reverse flow direction). The FFT window size was 128 point (17.9 ms) with Hanning window, and the 64-scale Morlet wavelet was used for the CWT.

scale points. Results obtained for the 128-point FFT, the 64-point FFT, and the CWT were compared using paired *t*-tests.

**RESULTS**

The Morlet wavelet increased embolic signal conspicuity assessed visually, compared with the FFT, and this was particularly marked for the shorter duration embolic signals, as demonstrated by the example shown in Figs. 2 and 3. Consistent with the visual assessment, the CWT had higher temporal resolution than either the 128- or 64-point FFTs, as evidenced by a significantly lower mean HWM (Table 1). Time localization using the CWT was also better than using the FFT and shows very close agreement with the measurement from the time-domain signal. In contrast, the FFT results in a mean time of onset by  $-5.9$  ms for 64-point FFT and  $-11.94$  for 128-point FFT (standard deviations were 2.1 and 3.17, respectively). Histograms illustrating the distributions of estimations of time localizations for the CWT and the 64-point FFT are shown in Fig. 4.

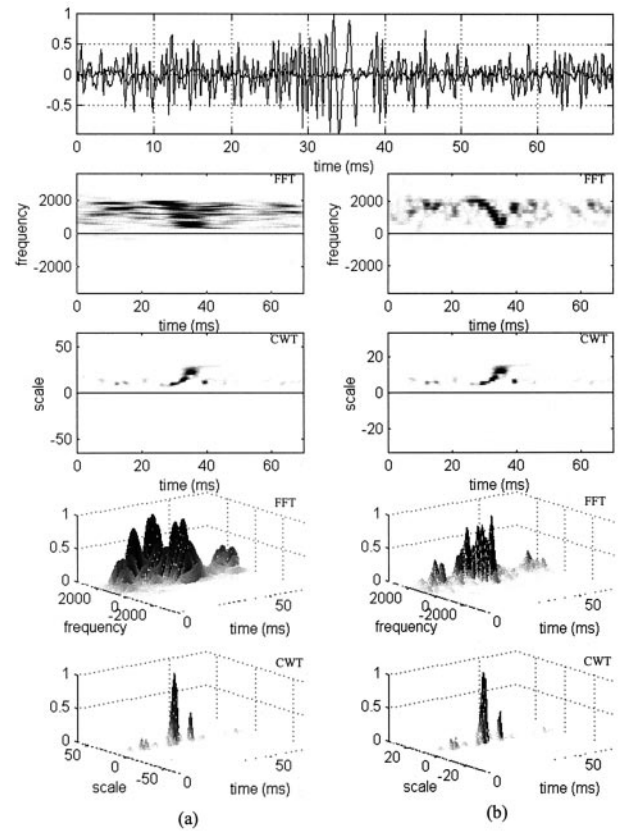


Fig. 3. A low-intensity embolic signal and corresponding 2-D and 3-D intensity plots of the FFT and the CWT results (– indicates reverse flow direction) for (a) the 128-point FFT and 64-scale CWT, (b) the 32-point FFT and 32-scale CWT.

The mean EBR for the CWT (16.94 dB, SD = 2.4) was slightly lower than the mean EBR for the 128-point FFT (17.11 dB, SD = 3) and slightly greater than the

Table 1. Mean and standard deviations (SD) of the EBR, HWM, and ESO for the 50 embolic signals

	EBR (dB), Mean (SD)	HWM (ms), Mean (SD)	ESO (ms), Mean (SD)
CWT (Morlet)	16.94 (2.4)	8.40 (8.82)	66.94 (8.57)
FFT (128-p)	17.11 (3.0)	12.92 (9.70)	54.05 (8.09)
FFT (64-p)	16.87 (2.65)	10.80 (5.69)	60.05 (8.59)
Time domain signal			65.96 (8.76)
2-tail Significance values			
CWT vs. FFT (128-p)	0.767	0.001	–
CWT vs. FFT (64-p)	0.918	0.006	–
FFT (128-p) vs. FFT (64-p)	0.020	0.001	–
ESOT vs. FFT (128-p)	–	–	0.001
ESOT vs. FFT (64-p)	–	–	0.001
ESOT vs. CWT	–	–	0.252

EBR = embolic signal power to averaged background ratio; HWM = half-width maximum; ESO = embolic signal onset; ESOT = embolic signal onset measured from the time domain signal.

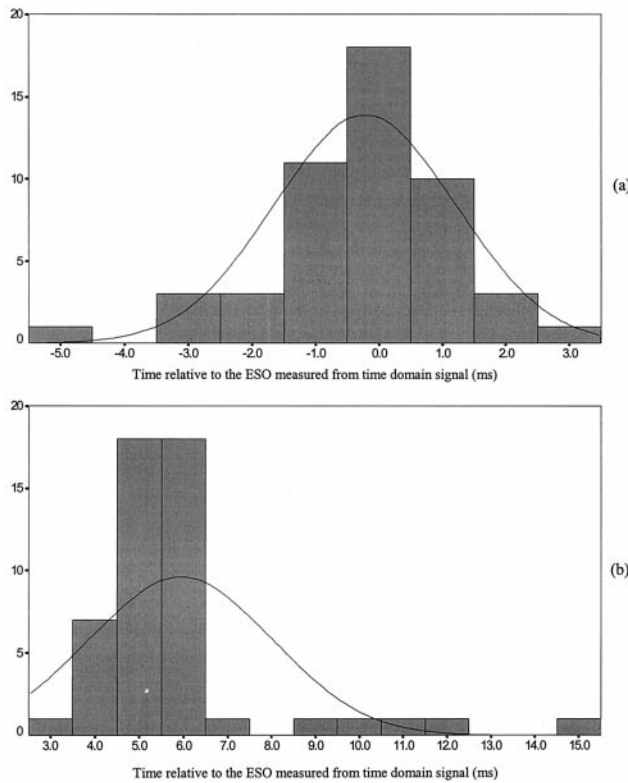


Fig. 4. Histograms illustrating the distributions of estimations of time localizations for (a) the CWT and (b) the 64-point FFT.

mean EBR with the 64-point FFT (16.87 dB, SD = 2.65), though these differences were not significant.

For the second group of 10 low-intensity embolic signals, the mean EBR for the CWT (11.37 dB, SD = 1.08) was not significantly higher than both the mean EBR for the 64-point FFT (11.16 dB, SD = 1.03,  $p = 0.310$ ) and the 128-point FFT (11.2 dB, SD = 1.4,  $p = 0.429$ ). For this second data set, we also studied the effect of using a shorter window length with a 16-point FFT. This resulted in a lower mean EBR of 9.7 dB (SD = 0.51,  $p = 0.001$  compared with CWT). Looking at this data set of low-intensity embolic signals, the time resolution was also as good or better for the CWT (mean 10.61 ms, SD = 6.94), compared with the 16-point FFT (10.82 ms, SD = 6.87,  $p = 0.864$ ), the 64-point FFT (11.81 ms, SD = 6.8,  $p = 0.191$ ) and the 128-point FFT (14.62 ms, SD = 6.94,  $p = 0.003$ ).

## DISCUSSION

The wavelet transform appears well suited to the analysis of embolic signals, offering superior time resolution and time localization compared to the FFT approach. Its use avoids the trade-off between frequency resolution and temporal resolution inherent in the appli-

cation of the FFT. Time localization of the FFT is very much dependent on the overlap ratio and the window size used, but commercial systems use the same window length as the FFT size and, therefore, we did not analyze the effect of different window sizes on the time localization and temporal resolution. Fortunately, the overlapping process introduces a predictable time shift on the actual location of an event on the time-frequency plane of the FFT. The duration of the time shift depends on the overlap ratio used, and the direction of the time shift is dictated by the way that the data are arranged prior to the FFT. If zeros are added to the end of the original data array and then the FFT is applied, the detection of embolic event leads the actual event. If zeros are added to the beginning of the original data array and then the FFT is applied, the detection of embolic event lags the actual event. Duration of the time shift can be estimated as  $(\text{number of overlapped samples}/2) \times \text{sampling time}$ . The time shift can be adjusted by adding zeros equally at both ends of the original data array. However, because commercial analysis software is not transparent to users, one should be very careful of interpretation of the time localization properties of the Fourier-based techniques. In addition, systems optimized for good frequency resolution introduce a spread on time localization. This also causes an overestimation of time localization of the FFT. On the other hand, the WT gives almost exact location and duration of the embolic signal inherently.

We studied embolic signals from patients with carotid stenosis. These embolic signals are of low intensity (Grosset *et al.* 1993), and are more difficult to detect using current automated detection systems based on FFT spectral processing (Van-Zuilen *et al.* 1996). Therefore, these are an appropriate sample on which to test a novel processing approach such as the wavelet transform, which may be particularly suited to short-duration low-intensity signals. As well as an unselected consecutive sample of embolic signals, we studied 10 low-intensity embolic signals that are at the lower range of those detectable using FFT analysis based on a standard transcranial Doppler system. The wavelet approach seemed particularly suited to the analysis of such signals.

For unselected embolic signals from patients with carotid stenosis, the mean EBR for the CWT was slightly lower than the mean EBR for the 128-point FFT, although the absolute differences were very small and not significant. However, using shorter windows for the FFT processing will result in a reduced EBR because it was noted that the EBR of the 64-point FFT was lower than that for the 128-point FFT. This is because the longer frame sizes will be less sensitive to sudden variations and will produce a smoother spectrum, but will cause a temporal smearing and blur transient events. This may be avoided by employing shorter windows. However, sig-

nal-to-noise ratio decreases with decreasing window duration (Pitton et al. 1996). The windowing function (Hanning) used prior to the FFT with a 99% overlap also suppresses and smoothes the background signal. For the low-intensity embolic signals, the mean EBR for the CWT was not significantly higher than both the mean EBR for the 128-point FFT and 64-point FFT.

An important consideration in automated embolic signal detection is the need for an online system. Inherently, the CWT is computationally intensive process because it is evaluated at each scale and, although it is possible to implement the CWT using parallel processing techniques, there are fast implementations of wavelet transform using filter banks (Strang and Nguyen 1997). This is called the fast wavelet transform (FWT) as an analogy to the fast Fourier transform (Cody 1992). The FWT is computationally very efficient and can be implemented in real-time easily using a DSP processor (Cody 1993).

The results obtained by the CWT heavily depend upon the choice of an appropriate wavelet. Using a more appropriate wavelet will result in higher amplitude wavelet coefficients and, hence, a higher EBR value. We selected the Morlet wavelet from those available in the Matlab signal-processing program because it best described embolic signals. However, it may be possible to construct a better wavelet that will more accurately describes such signals and result in a higher EBR. Nevertheless, this study with a standard wavelet transform suggests that the wavelet approach is well suited to analyze the short-duration embolic signals.

*Acknowledgements*—This work was supported by a British Heart Foundation project grant (PG96176). We are grateful to Marisa Cullinane for assistance in analyzing data, Kamran Modaresi for advice on computing aspects and William J. Williams for useful comments on the manuscript.

## REFERENCES

- Akay M. Wavelets in biomedical engineering. *Ann Biomed Eng* 1995; 23:531–542.

- Aydin N, Fan L, Evans DH. Quadrature-to-directional format conversion of Doppler signals using digital methods. *Physiol Meas* 1994; 15:181–199.
- Chan CBC, Chan FHY, Lam FK, Lui PW, Poon PWF. Fast detection of venous air embolism in Doppler heart sound using the wavelet transform. *IEEE Trans Biomed Eng* 1997;44:237–245.
- Cody MA. The fast wavelet transform: Beyond Fourier transforms. *Dr Dobb's J* 1992;April:16–28.
- Cody MA. A wavelet analyser: An alternative to the FFT-based spectrum analyzer. *Dr Dobb's J* 1993;April:44–54.
- Farge M. Wavelet transforms and their applications to turbulence. *Annu Rev Fluid Mech* 1992;24:395–457.
- Grosset DG, Georgiadis D, Kelman AW, Lees KR. Quantification of ultrasound embolic signals in patients with cardiac and carotid disease. *Stroke* 1993;24:1922–1924.
- Markus HS, Harrison MJ. Microembolic signal detection using ultrasound. *Stroke* 1995;26:1517–1519.
- Markus HS, Tegeler C. Experimental aspects of high-intensity transient signals in detection of emboli. *J Clin Ultrasound* 1995;23:81–87.
- Markus HS, Ackerstaff R, Babikian V, Bladin C, Droste D, Grosset D, Levi C, Russell D, Siebler M, Tegeler C. Inter-centre agreement in reading Doppler embolic signals: a multicentre international study. *Stroke* 1997;28:1307–1310.
- Martinet RK, Morlet J, Grossmann A. Analysis of sound patterns through wavelet transforms. *Intl J Pattern Recogn Artificial Intellig* 1986;1:273–302.
- Pitton JW, Wang K, Juang BH. Time-frequency analysis and auditory modelling for automatic recognition of speech. *Proc IEEE* 1996; 84:1199–1215.
- Ringlestein EB, Droste DW, Babikian VL, Evans DH, Grosset DG, Kaps M, Markus HS, Russell D, Siebler M, International Consensus Group on Microembolus Detection. Consensus on microembolus detection by TCD. *Stroke* 1998;29:725–729.
- Rioul O, Vetterli M. Wavelets and signal processing. *IEEE Signal Proc Magazine* 1991;8:14–38.
- Smith JL, Evans DH, Fan L, Thrush AJ, Naylor AR. Processing Doppler ultrasound signals from blood born-emboli. *Ultrasound Med Biol* 1994;20:455–462.
- Spencer MP, Thomas GI, Nicholls SC, Sauvage LR. Detection of middle cerebral emboli during carotid endarterectomy using transcranial Doppler ultrasonography. *Stroke* 1990;21:415–423.
- Strang G, Nguyen T. *Wavelets and filter banks*. Wellesley: Wellesley-Cambridge Press, 1997.
- Torrence C, Compo GP. A practical guide to wavelet analysis. *Bull Am Meteor Soc* 1998;79:61–78.
- Van-Zuilen EV, Mess WH, Jansen C, Van-der-Tweel I, Van-Gijn J, Ackerstaff RGA. Automatic embolus detection compared with human experts: A Doppler ultrasound study. *Stroke* 1996;27:1840–1843.
- Williams WJ, Sang T, O'Neill JC, Zalubas EJ. Wavelet windowed time-frequency distribution decompositions. *SPIE* 1997;3162:149–160.